

Substrate Inhibition in the Heterogeneous Catalyzed Aldol Condensation: A Mechanistic Study of Supported Organocatalysts

Kapil Kandel,^{a,b} Stacey M. Althaus,^{a,b} Chorthip Peeraphatdit,^{a,b} Takeshi Kobayashi,^a
Brian G. Trewyn,^b Marek Pruski,^{a,b} Igor I. Slowing^{a*}

^aU.S. Department of Energy, Ames Laboratory, Ames, Iowa, U.S.A. 50011-3020

^bDepartment of Chemistry, Iowa State University, Ames, Iowa, U.S.A. 50011-3111

Abstract

In this study we demonstrate how materials science can be combined with the established methods of organic chemistry to find mechanistic bottlenecks and redesign heterogeneous catalysts for improved performance. By using solid-state NMR, infrared spectroscopy, surface and kinetic analysis, we prove the existence of a substrate inhibition in the aldol condensation catalyzed by heterogeneous amines. We show that modifying the structure of the supported amines according to the proposed mechanism dramatically enhances the activity of the heterogeneous catalyst. We also provide evidence that the reaction benefits significantly from the surface chemistry of the silica support, which plays the role of a co-catalyst, giving activities up to two orders of magnitude larger than those of homogeneous amines. This study confirms that the optimization of a heterogeneous catalyst depends as much on obtaining organic mechanistic information as it does on controlling the structure of the support.

Keywords: Mesoporous silica nanoparticles; Heterogeneous catalysis; Aldol condensation; Substrate inhibition; Cooperative catalysis; Solid-state NMR

1. Introduction

One of the characteristics that distinguish homogeneous from heterogeneous catalysis is the intricacy of the reaction environment. The uniform nature of homogeneous catalysts facilitates identification of intermediates and enables understanding of the transformations in terms of reaction mechanisms. This permits optimization of the activity by slight variations to the molecular structure of the catalyst.[1] Unraveling of reaction mechanisms in heterogeneous catalysis poses additional challenges due to the different environments that the active sites can encounter on a solid support. Therefore, optimization of heterogeneous catalysts is often performed by selection or design of supports rather than by modifying the structure of the catalytic groups.[2-5] In addition, homogeneous catalysts typically exhibit superior selectivity and kinetics. Despite these disadvantages, heterogeneous catalysts are valued because they allow easy separation of products and can be reused for extended periods of time.[6]

Given its importance as a C-C bond-forming reaction, the aldol condensation has been a common target for catalyst design.[7-11] This reaction is performed in organisms by aldolases, which activate donor ketones with the amino group of a highly conserved lysine, to give enamines. The enamines attack aldehyde acceptors and are then hydrolyzed to release the product.[12, 13] Homogeneous catalysis of this reaction has been accomplished by strong acids or bases, combining nucleophilic addition with enolization,[14, 15] and recently by proline and catalytic antibodies.[16, 17] Many heterogeneous catalysts have been developed to promote this reaction, and among those with organic groups as active sites, the most commonly used are aminoalkyls.[18-24]

While supported aminoalkyls promote the aldol condensation, their catalytic efficiency is relatively low.[20, 21, 23-27] A way to solve this problem could be by

introducing a secondary functional group in the material.[28] Davis and co-workers adopted this strategy and synthesized a bifunctional catalyst by introducing amine and sulfonic acid groups on mesoporous silica, which dramatically increased the activity due to cooperativity between both groups.[25, 26] Solin and collaborators, as well as Thiel and co-workers, obtained similar results, using different combinations of alkylamines and acidic groups in mesoporous silica supports.[23, 27] However, the poor catalytic activity of monofunctional amine on silica, which remains commonly used for the aldol and similar types of condensation, [20, 22, 24, 29-32] is still not well understood.

Herein, we investigate in detail the mechanistic causes of the poor catalytic activity of amine functionalized mesoporous silica towards the aldol condensation. Based on this understanding we demonstrate that the performance can be dramatically improved by the proper choice of the catalytic groups. Furthermore, we report activities that surpass those observed in the homogeneously catalyzed reactions, and demonstrate that these enhanced activities arise from the cooperative interactions between organocatalysts and the support.

2. Materials and Methods

2.1 Materials

Cetyltrimethylammonium bromide (CTAB), mesitylene, p-nitrobenzaldehyde, hexamethyldisilazane (HMDS) and dimethyl sulfone were purchased from Sigma-Aldrich. Tetraethylorthosilicate (TEOS), 3-aminopropyl trimethoxysilane, [3-(Methylamino)propyl] trimethoxysilane and [3-(N,N-Dimethylamino)propyl] trimethoxysilane were purchased from Gelest. All reagents were used as received without further purification.

2.2 Synthesis of Amine-Functionalized Mesoporous Silica Nanoparticles

The functionalized mesoporous silica nanoparticles (MSNs) with particle sizes ranging from 80 to 150 nm (Figure S1) were prepared following a previously published method.[33] CTAB (1.0 g, 2.7 mmol) was dissolved in nanopure water (480 g, 26.7 mol), followed by the addition of NaOH solution (2.0 M, 3.5 mL, 7.0 mmol). The mixture was heated to 80 °C for 1 h. To this clear solution, TEOS (4.7 g, 23 mmol) was added drop wise, followed by immediate addition of 3-aminopropyl trimethoxysilane (for AP-MSN) (1.0 mL, 5.7 mmol) and [3-(Methylamino)propyl] trimethoxysilane (for MAP-MSN) (1.0 mL, 5.0 mmol). The reaction mixtures were stirred vigorously at 80°C for 2 h and then filtered to yield white functionalized solids. The as-synthesized materials were washed with copious amounts of water and methanol, and then dried under vacuum. The final catalysts were obtained by removing the CTAB surfactant via Soxhlet extraction with methanol for 24 h, followed by drying overnight under vacuum. These samples were labeled AP-MSN-2.8 and MAP-MSN-2.6, based on the average pore size (2.8 nm and 2.6 nm, respectively).

2.3 Synthesis of Pore-Expanded Functionalized Mesoporous Silica Nanoparticles

The functionalized MSN materials with larger pores (AP-MSN-3.6 and MAP-MSN-3.5) were prepared following the same procedure as described above, except for the initial step which involved adding the pore expander agent mesitylene (1.73 g, 14.4 mmol) to the original CTAB solution, as previously published.[34] A third pore-expanded catalyst was also prepared functionalized with [3-(N,N-Dimethylaminopropyl)] trimethoxysilane (1.0 mL, 4.6 mmol) and labeled DMAP-MSN-3.2.

2.4 Passivation of MAP-MSN-3.5 material

The silylation was performed by placing 1.0 g of MAP-MSN-3.5 material in a hexane solution of hexamethyldisilazane (HMDS) (100 mL hexane, 10 mmol HMDS).[35],[36] The mixture was refluxed for 24 h, the resulting solution was then filtered, washed three times with hexane, and dried under vacuum.

2.5 Characterization

The surface areas and pore size distributions of the catalysts were measured by nitrogen sorption isotherms in a Micromeritics Tristar analyzer, and calculated by the Brunauer-Emmett-Teller (BET) and Barrett-Joyner-Halenda (BJH) methods, respectively (Table S1). The transmission electron microscopy (TEM) examination was completed on a Tecnai G2 F20 electron microscope operated at 200 kV (Figure S1). For the TEM measurements, an aliquot of the powder was sonicated in methanol for 15 min. The small angle powder X-ray diffraction patterns were obtained with a Rigaku Ultima IV diffractometer using Cu target at 40 kV and 44 mA (Figure S2). The Cu K β radiation was removed using a monochromator. A single drop of this suspension was placed on a lacey carbon coated copper TEM grid and dried in air. Fourier transform infrared (FT-IR) spectra were recorded on Nicolet Nexus 470. Solid-state NMR experiments are described separately below. Loading of the catalytic groups was measured by elemental analysis in a Perkin Elmer 2100 Series II CHN/S Analyzer, with acetanilide as calibration standard, and combustion and reduction temperatures of 925 °C and 640 °C. The expected precision and accuracy of the analysis was $\pm 0.3\%$ for each element, each material was tested by triplicate.

2.6 General Procedure for Aldol Condensation Reaction

All catalytic reactions were performed in screw-cap vials. *p*-nitrobenzaldehyde (0.39 mmol) was dissolved in acetone (1.5 mL). To this solution, a suspension of the

catalyst containing 0.0117 mmol of the amine group (corresponding to 3 mol% of the *p*-nitrobenzaldehyde) in hexane (1.5 mL) was added. The solution was stirred at 60°C for specified times and set on ice to quench the reaction. The catalyst was separated by centrifugation and the supernatant was concentrated under reduced pressure. The yield of the products was determined by ¹H NMR, using dimethyl sulfone as an internal standard.

2.7 Solid-State NMR

Solid-state NMR experiments were used to determine the structures of surface bound species and intermediates. This technique was also used as an additional tool to evaluate the loading of the functional groups on the MSN surface by means of ²⁹Si spectra, measured using direct polarization (DP) under magic angle spinning (MAS) with Carr-Purcell-Meiboom-Gill (CPMG) refocusing of ²⁹Si magnetization,[37] as previously described (Table S1).[38]

¹³C cross polarization (CP) MAS spectra were used to verify the structure of the functional groups and to determine the identities of intermediates formed in the AP-MSNs. These experiments were performed at 9.4 T on a Chemagnetics Infinity 400 spectrometer equipped with a 5-mm MAS probe operated at 400.0 MHz (¹H) and 79.4 MHz (²⁹Si), and at 14.1 T on a Varian NMR System 600 spectrometer equipped with a 1.6-mm FastMASTM probe operated at 599.6 MHz (¹H) and 150.8 MHz (¹³C).

Experimental parameters are given below using the following symbols: v_R denotes the MAS rate, $v_{RF}(X)$ the magnitude of radiofrequency magnetic field (RF) applied to X spins, τ_{CP} the mixing time during cross polarization, N_{CPMG} the number of CPMG echoes, τ_{RD} the recycle delay, NS the number of scans, and AT the total acquisition time.

^{29}Si DPMAS with CPMG: $\nu_{\text{R}} = 10 \text{ kHz}$, $\nu_{\text{RF}}(^{29}\text{Si}) = 50 \text{ kHz}$, $\nu_{\text{RF}}(^1\text{H}) = 45 \text{ kHz}$, $N_{\text{CPMG}} = 10$, $\tau_{\text{RD}} = 300 \text{ s}$, $\text{NS} = 296$, and $\text{AT} = 25 \text{ h}$.

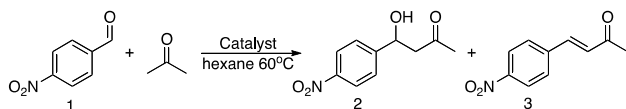
^{13}C CPMAS: $\nu_{\text{R}} = 40 \text{ kHz}$, $\nu_{\text{RF}}(^{13}\text{C}) = 140 \text{ kHz}$, $\nu_{\text{RF}}(^1\text{H})$ during CP = 60 kHz , $\nu_{\text{RF}}(^1\text{H})$ during SPINAL-64 decoupling = 12 kHz , $\tau_{\text{CP}} = 3 \text{ ms}$, $\tau_{\text{RD}} = 2 \text{ s}$, $\text{NS} = 26,400$, and $\text{AT} = 15 \text{ hrs}$.

The chemical shifts of ^{29}Si , ^{13}C and ^1H are reported using the δ scale and are referenced to tetramethylsilane (TMS) at 0 ppm.

3. Results and Discussion

3.1 Catalytic Activity of Homogeneous and Heterogeneous Propylamine

To set a reference, we measured the activity of propylamine as a homogenous catalyst for the cross-aldol condensation between *p*-nitrobenzaldehyde **1** and acetone at 60°C in hexane (Scheme 1). Catalytic activity was determined by measuring the formation of the aldol **2** and the α,β -unsaturated carbonyl **3** products. Consistent with the report by Davis and co-workers, homogenous propylamine displayed poor activity with only 4.5% conversion after 2 h.[25] Interestingly, while Davis observed a fourfold increase in yield upon supporting the amine on mesoporous silica,[25] the activity of our 3-aminopropyl-mesoporous silica nanoparticle catalyst with 2.8 nm pores (AP-MSN-2.8) was even lower than that of the homogeneous amine, giving only 2% conversion after 2 h.



Scheme 1. Cross-aldol condensation between *p*-nitrobenzaldehyde **1** and acetone.

Considering that the pores of AP-MSN-2.8 were smaller than those previously used (6.3 nm),[25, 39] we examined the activity of an AP-MSN-3.6 catalyst (with 3.6 nm wide pores). Remarkably, we found that this small increase in pore size, from 2.8 nm to 3.6 nm, led to a 20-fold increase in activity: the 2 h yield rose from 2% to 47%. The apparent pseudo first order rate constant of AP-MSN-3.6 ($k = 3.7 \times 10^{-1} \text{ h}^{-1}$) was two orders of magnitude larger than that of the homogeneous propylamine ($k = 2.6 \times 10^{-3} \text{ h}^{-1}$). This large change in activity suggested that the rate of the reaction was limited by the molecular diffusion within the narrower pores. However, the longest dimensions of the reactants and products (0.4 nm for acetone, 0.6 nm for **1**, and 1 nm for **2** or **3**) were small compared to the pore diameters of AP-MSN-2.8 and AP-MSN-3.6. Therefore, diffusion could not be the only factor limiting the catalytic activity.

When comparing the properties of AP-MSN-2.8 before and after the reaction, we discovered that despite the surface area of the material remaining relatively constant (906 m²/g before and 894 m²/g after the reaction), the pore size decreased significantly to 2.0 nm. In addition, we observed an inhibition of the reaction kinetics at high concentrations of substrate **1** (Figure 1). The Lineweaver-Burk plot of the data obtained at concentrations lower than 100 mM gave a Michaelis-Menten constant (K_M) of 273 and a maximal rate (V_{\max}) of 0.594 mmol h⁻¹ ($r^2 = 0.9992$) (Figure S3). These estimates are clearly larger than the experimental values, and therefore indicate a strong substrate inhibition.[27, 40] These results suggested that the catalytic sites of the material could be blocked by the formation of a stable Schiff base, which has been reported to inhibit the aldol condensation by catalytic antibodies (Scheme 2).[41, 42]

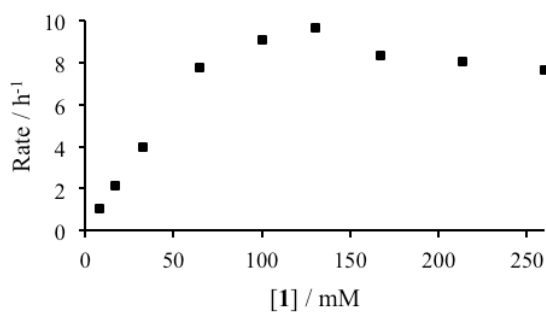
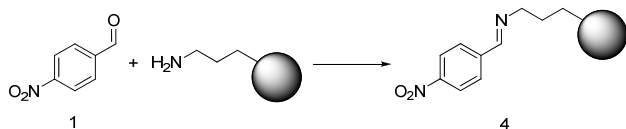


Figure 1. Effect of substrate concentration on the rate of AP-MSN-3.6 catalyzed cross-aldol condensation. The drop in rate at high concentrations of **1** suggests substrate inhibition of the reaction.



Scheme 2. Formation of a Schiff base between p-nitrobenzaldehyde substrate **1** and the aminopropyl group of AP-MSN.

3.2 Detection of Inhibition Intermediate

Although it has been suggested that an imine could form during the aldol condensation catalyzed by AP-MSN, no direct evidence has been provided for its existence.[23] When comparing the infrared and NMR spectra of AP-MSN-2.8 before and after the reaction we confirmed the formation of imine intermediate **4**, which was stable even after washing and drying the material. While the C-C stretching *e2g* band (1606 cm⁻¹) and the symmetric and asymmetric stretching bands of -NO₂ (1345 cm⁻¹, 1537 cm⁻¹) of **1** could be clearly identified in AP-MSN-2.8 following the reaction, the stretching frequency of C=O (1706 cm⁻¹) was no longer visible, but was replaced with a signal at 1646 cm⁻¹ corresponding to the C=N stretching of the imine (Figure 2a). Solid-state ¹³C NMR spectroscopy unambiguously confirmed the formation of **4**

(Figure 2b). The resonance of carbon 'c' in AP-MSN-2.8 decreased considerably after the reaction, giving rise to a resonance at 160 ppm corresponding to the C=N carbon ('d') in **4**, whereas no signal due to the carbonyl carbon of **1** (190 ppm) was observable. A strong downfield shift of the resonance of C-3 in AP-MSN (resonance 'c' shifting to 'c*') was also observed after the reaction with **1** (Figure 2b). This suggested a chemical transformation of the aminopropyl group rather than a mere physisorption of **1** to the surface of the particles. A fraction of unreacted aminopropyl was still visible in the sample as shown by resonance 'c' in the used catalyst. Comparison of nitrogen content of the material before and after the reaction by elemental analysis revealed that approximately 70% of amine groups formed the imine. Although the ^{13}C CPMAS spectra in Figure 2b are not strictly quantitative, the intensity ratio of resonances 'c*' and 'c' is in approximate agreement with the elemental analysis.

Treatment of the poisoned AP-MSN catalyst with 0.01 M HCl for 24 h at room temperature led to hydrolysis of the Schiff base, as evidenced by disappearance of the signals of **4** in the infrared and NMR spectra of the treated material. The regeneration of AP-MSN catalyst was also confirmed by elemental analysis: the number of mmol of nitrogen per gram of material varied from 1.0 before reaction to 1.7 after formation of **4**, to 1.16 after treatment with dilute acid.

The relatively large size of the Schiff base **4** (about 1 nm) explained the reduction in the pore size of AP-MSN by 0.8 nm, as well as the dramatic effect of the small increase in pore size on the reaction yield. The inhibition at high concentrations of **1** suggested the mechanism of the reaction is unlikely Mannich type, but should involve either enamine or enolate intermediates.

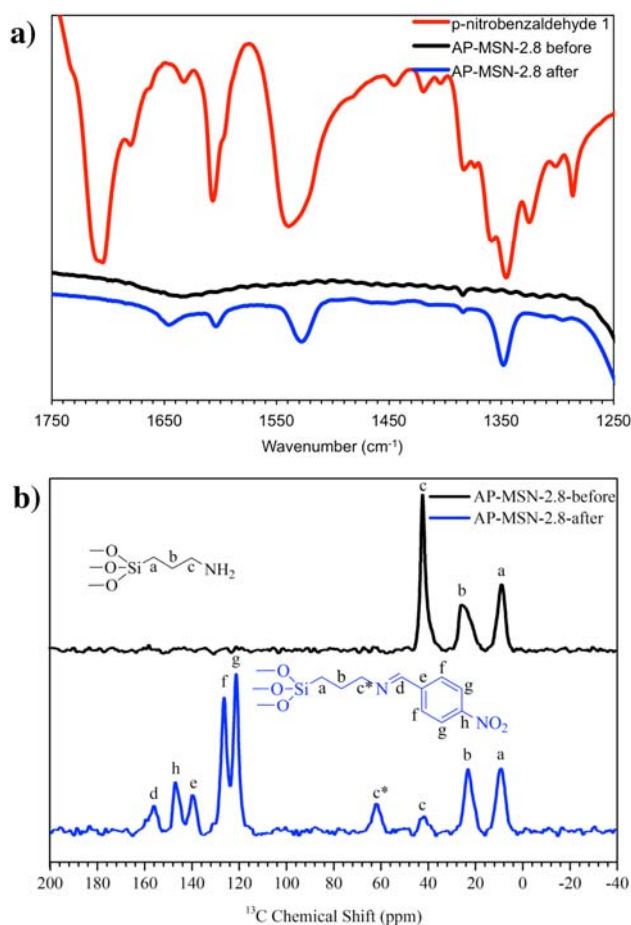


Figure 2. Infrared (a) and ¹³C CPMAS NMR (b) spectra of AP-MSN-2.8 before (black) and after (blue) reaction with **1**. Infrared spectrum of **1** (red) is included as a reference.

3.3 Structural Modification of the Catalytic Group

Based on the hypothesis that the low activity of AP-MSN was caused by the formation of a stable Schiff base, we functionalized the MSNs with a secondary amine, which is unable to form imines. Two catalysts containing 3-(N-methylamino)propyl (MAP) with different pore sizes were prepared (MAP-MSN-2.6 and MAP-MSN-3.5) and tested for the reaction. As expected, no imine was detected by infrared and NMR analyses of MAP-MSNs after the reaction. Remarkably, even the narrow-pore MAP-MSN-2.6 doubled the activity of the wide-pore AP-MSN-3.6, yielding 93% conversion

after 2 h. Also, no inhibition of reaction kinetics was observed at high concentrations of **1** (Figure S4). The conversion using MAP-MSN-3.5 was further elevated to 97%. These results suggested that imine formation with AP-MSN catalysts lowered the activity by blocking diffusion and by reducing the number of active sites.

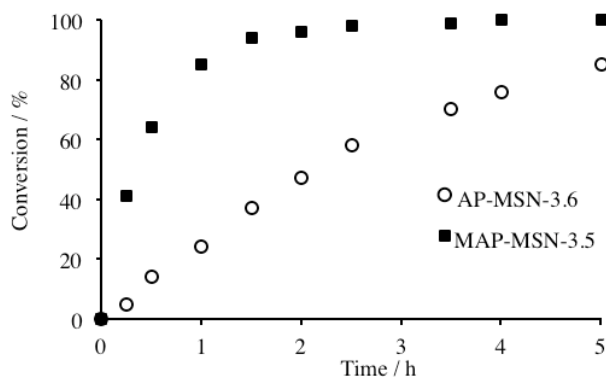


Figure 3. Kinetics of aldol condensation between **1** and acetone catalyzed by AP-MSN-3.6 and MAP-MSN-3.5 in hexane at 60°C with 3 mol% catalyst.

We also noted that the apparent rate constant of MAP-MSN-3.5 ($k = 1.35 \text{ h}^{-1}$) was over three times larger than that of AP-MSN-3.6 ($k = 0.37 \text{ h}^{-1}$) (Figures 3 and S5). We considered the possibility that the increase in catalytic activity could be due to MAP-MSN being more nucleophilic or basic than AP-MSN. This could imply a mechanism involving enolates rather than enamines. Although unlikely, due to the high $\text{p}K_{\text{b}}$ of amines, we tested this hypothesis by preparing a new material functionalized with a tertiary amine. The material containing 3-(N,N-dimethylamino)propyl group (DMAP-MSN-3.2), failed to catalyze the reaction, proving that the conversion is not promoted by simple deprotonation. It must be pointed out that, being a tertiary amine, DMAP cannot form an enamine, which is consistent with the reaction proceeding through an enamine pathway.

We finally noted that the MAP-MSN catalysts are significantly more active than the previously reported amphoteric bifunctional catalysts, giving higher conversion in only 2 h than the bifunctional catalysts gave over 20 h of reaction.[25, 39, 43]

3.4 Cooperative Effects of the Support

Having established the role of the catalytic groups, we focused on the role of the support. As in the case of AP-MSN-3.6, the activity of the heterogeneous MAP-MSN-3.5 catalyst ($k = 1.35 \text{ h}^{-1}$) is much higher than that of the corresponding homogeneous catalyst N-methyl-propylamine ($k = 0.056 \text{ h}^{-1}$) (Figure S5). These unusual results contradict the general observation that homogeneous catalysis is much faster than heterogeneous catalysis,[44] and suggest that the support plays an active role in the reaction mechanism. Indeed, the weakly acidic silanol groups on the surface of silica have been previously recognized as capable of assisting various reactions.[23, 45-49]

To test the participation of silanol groups in the catalytic process, we treated MAP-MSN-3.5 with hexamethyldisilazane (HMDS). ^{29}Si NMR showed that this reduced the number of silanols by 39% (from 3.8 to 2.3 mmol/g, Figure 4). When using this passivated catalyst the yield of the reaction dropped by 34% (from the original 97% to 63%). Furthermore, addition of non-functionalized MSN to homogeneous N-methyl-propylamine increased the conversion to 51% compared to the 10% yield observed when using only the homogeneous catalyst (Figure 5). These results confirm not only that the silanol groups play an active role in the catalytic process, but also that their proximity to the amine sites is beneficial, which suggests a cooperativity between both groups.

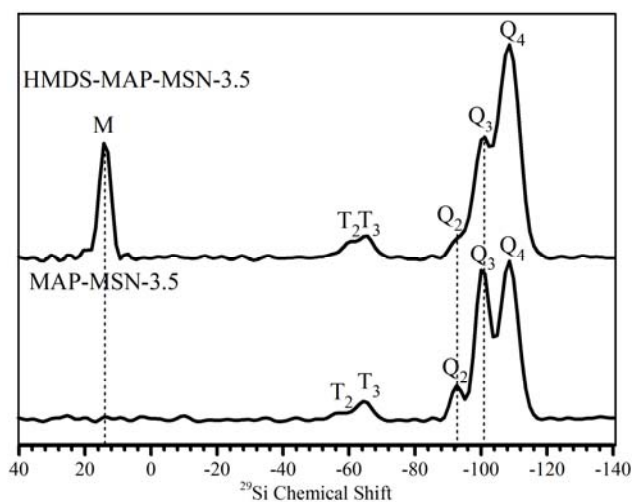


Figure 4. ^{29}Si DPMAS spectra of MAP-MSN-3.5 before (bottom) and after (top) blocking silanol groups with HMDS. Appearance of M sites due to the attached silane matches the conversion of the Q_2 and Q_3 sites of the blocked groups to Q_3 and Q_4 , respectively.[50]

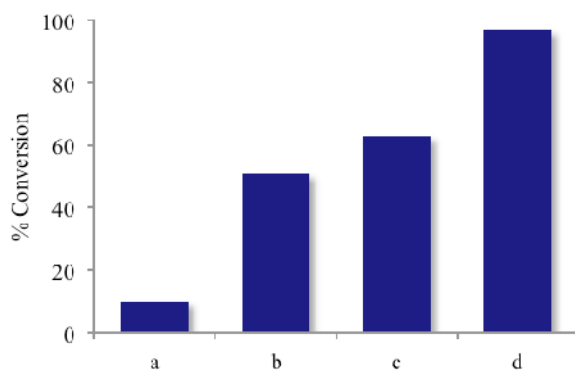
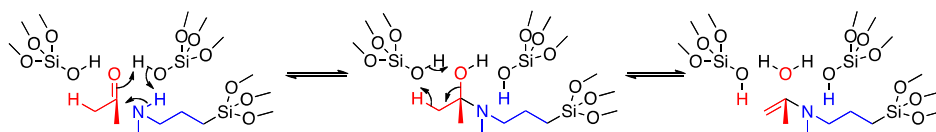


Figure 5. Effect of proximity between silanol and amine groups on the conversion of *p*-nitrobenzaldehyde. Catalytic activities are compared for: (a) homogeneous N-methyl-propylamine, (b) homogeneous N-methyl-propylamine + heterogeneous MSN, (c) silanol-passivated HMDS-MAP-MSN-3.5, and (d) heterogeneous MAP-MSN-3.5.

The role of silanols in the reaction can be explained by the fact that carbonyl compounds adsorb on the surface of silica via hydrogen bonding.[26, 51-56] We confirmed this interaction by measuring NMR spectrum of ^{13}C -labeled acetone set in contact with non-functionalized MSN (Figure S6), which exhibited a downfield shift of the carbonyl carbon signal compared to that of neat acetone (~213 ppm versus 206 ppm). Our earlier solid-state NMR and theoretical studies demonstrated that surface silanols on silica also interact with the amine functionalities.[57] These findings suggest that silanol groups play a key role in bringing all reactants and the catalytic group together for the reaction to take place. In contrast, the probability of bringing acetone, the aldehyde and the amine catalyst together is dramatically decreased in the homogeneous medium. Similarly, the probability of encounter must be lower if the amine is not covalently attached to the silica support. This explains the observed activity trend: homogeneous MAP < MAP + MSN < MAP-MSN (Figure 5). In addition, when introducing DMSO (hydrogen bond-acceptor, $\alpha = 0.00$, $\beta = 0.76$)[23, 58] to the reaction, we observed a significant drop in the conversion catalyzed by MAP-MSN-3.5, from 97% to 55%. This drop can be attributed to the competition of DMSO with the reactants for hydrogen-binding the silanol groups.

The formation of hydrogen bonds between silanols and carbonyls may also contribute to the activation of the latter for nucleophilic attack by the amine, and may assist in the formation of the reaction intermediate by facilitating the departure of carbonyl oxygen as water (Scheme 3). The formation of the intermediate enamine involves a series of proton transfers, which may be difficult to achieve in a non-polar medium. The mildly acidic silanol groups could assist these transfers by aligning with acetone and amine groups in six-membered ring-like arrangements, as in the Zimmerman-Traxler model (Scheme 3).[59, 60] For these intermediates to form, the

silanol groups should be as close as 5 to 6 Å from each other. As mentioned earlier, ^{29}Si NMR spectroscopy of MAP-MSN revealed a silanol content of 3.8 mmol/g (Figure 4), which at a surface area of 937 m^2/g gives a silanol density of 2.4 groups/ nm^2 . This density satisfies the inter-silanol distance required for the cyclic model. A third silanol group could also be closely located to this intermediate, providing a site for hydrogen bonding of **1**, to complete the reaction by a similar proton transfer process.



Scheme 3. Possible pathway of proton transfer assisted by silanol groups.

We also observed that the immobilization on silica led to a larger increase in the activity of the primary amine than the secondary amine ($k_{\text{het}}/k_{\text{homo AP}} = 142$, $k_{\text{het}}/k_{\text{homo MAP}} = 23$). This significant difference suggests that silanol groups may play yet another role in the catalysis. As mentioned above, the low catalytic activity of propylamine and AP-MSNs is attributed to the formation of a stable imine. Since imine hydrolysis is catalyzed by acids,[61] it is likely that the weakly acidic silanols assist the hydrolysis of a fraction of the imines, thus giving an additional advantage to AP-MSN compared to homogeneous propylamine. This would also explain, in part, the enhanced activity observed upon co-functionalization of aminopropyl mesoporous silica with acidic groups, as previously reported by Davis and Solin.[25-27]

4. Conclusions

In conclusion, the poor catalytic activity of aminopropyl functionalized mesoporous silica for the aldol condensation arises from a substrate inhibition. This inhibition takes place by formation of a stable Schiff base, which not only eliminates active sites but also blocks diffusion in pores 2.8 nm or smaller. This inhibition can be partially reduced by increasing the pore size of the support, or eliminated by modifying the structure of the amine from primary to secondary.

The silanol groups in the support assist the catalytic activity of immobilized amines by offering binding sites for the reactants in close proximity to the amines, providing pathways for proton transfer throughout all the steps of the reaction, and facilitating the departure of water during the formation of intermediates. This cooperation between the silica support and the amines dramatically improves the activity of the heterogeneous catalysts in comparison to the homogeneous catalysts in solution.

In summary, we have shown that heterogeneous organocatalysts are not only amenable to conventional mechanistic studies, but that the understanding achieved through these type of studies can guide their rational design to significantly improve their activity.

Acknowledgements

This research is supported by the U.S. Department of Energy, Office of Basic Energy Sciences, Division of Chemical Sciences, Geosciences, and Biosciences through the Ames Laboratory. The Ames Laboratory is operated for the U.S. Department of Energy by Iowa State University under Contract No. DE-AC02-07CH11358.

Supplementary data available.

References

- [1] B. Cornils, W.A. Herrmann, *J. Catal.*, 216 (2003) 23.
- [2] F. Rodríguez-Reinoso, *Carbon*, 36 (1998) 159.
- [3] X. Yu, X. Yu, S. Wu, B. Liu, H. Liu, J. Guan, Q. Kan, *J. Solid State Chem.*, 184 (2011) 289.
- [4] C.M.A. Parlett, D.W. Bruce, N.S. Hondow, A.F. Lee, K. Wilson, *ACS Catal.*, (2011) 636.
- [5] J.N. Stuecker, J.E. Miller, R.E. Ferrizz, J.E. Mudd, J. Cesarano, *Ind. Eng. Chem. Res.*, 43 (2003) 51.
- [6] A. Corma, H. Garcia, *Top. Catal.*, 48 (2008) 8.
- [7] H. Hattori, *Chem. Rev.*, 95 (1995) 537.
- [8] K.K. Rao, M. Gravelle, J.S. Valente, F. Figueras, *J. Catal.*, 173 (1998) 115.
- [9] H. Matsushashi, H. Miyazaki, Y. Kawamura, H. Nakamura, K. Arata, *Chem. Mater.*, 13 (2001) 3038.
- [10] D. Tichit, B. Coq, S. Cerneaux, R. Durand, *Catal. Today*, 75 (2002) 197.
- [11] T.R. Gaydhankar, P.N. Joshi, P. Kalita, R. Kumar, *J. Mol. Catal. A: Chem.*, 265 (2007) 306.
- [12] F. Tanaka, R. Fuller, H. Shim, R.A. Lerner, C.F. Barbas III, *J. Mol. Biol.*, 335 (2004) 1007.
- [13] F. Tanaka, R. Fuller, C.F. Barbas III, *Biochem.*, 44 (2005) 7583.
- [14] M. Chatterjee, K. Matsushima, Y. Ikushima, M. Sato, T. Yokoyama, H. Kawanami, T. Suzuki, *Green Chem.*, 12 (2010) 779.
- [15] S. Mukherjee, J.W. Yang, S. Hoffmann, B. List, *Chem. Rev.*, 107 (2007) 5471.
- [16] B. List, R.A. Lerner, C.F. Barbas III, *J. Am. Chem. Soc.*, 122 (2000) 2395.
- [17] S.M. Dean, W.A. Greenberg, C.-H. Wong, *Adv. Synth. Catal.*, 349 (2007) 1308.
- [18] Sujandi, S.-E. Park, D.-S. Han, S.-C. Han, M.-J. Jin, T. Ohsuna, *Chem. Commun.*, (2006) 4131.
- [19] S. Luo, J. Li, L. Zhang, H. Xu, J.-P. Cheng, *Chem. Eur. J.*, 14 (2008) 1273.
- [20] S. Luo, X. Zheng, J.-P. Cheng, *Chem. Commun.*, (2008) 5719.
- [21] T.M. Suzuki, M. Yamamoto, K. Fukumoto, Y. Akimoto, K. Yano, *J. Catal.*, 251 (2007) 249.
- [22] K.K. Sharma, T. Asefa, *Angew. Chem.*, 119 (2007) 2937.
- [23] S. Shylesh, A. Wagner, A. Seifert, S. Ernst, W.R. Thiel, *Chem. Eur. J.*, 15 (2009) 7052.
- [24] B. Liu, S. Wu, X. Yu, J. Guan, Q. Kan, *J. Coll. Interface Sci.*, 362 (2011) 625.
- [25] R.K. Zeidan, S.-J. Hwang, M.E. Davis, *Angew. Chem. Int. Ed.*, 45 (2006) 6332.
- [26] M. Wiesner, G.g. Upert, G. Angelici, H. Wennemers, *J. Am. Chem. Soc.*, 132 (2009) 6.
- [27] D.E. Purich, *Enzyme Kinetics: Catalysis and Control*, Elsevier, 2002.
- [28] J. Alauzun, A. Mehdi, C. Reye, R.J.P. Corriu, *J. Am. Chem. Soc.*, 128 (2006) 8718.
- [29] B.M. Choudary, M.L. Kantam, P. Sreekanth, T. Bandopadhyay, F. Figueras, A. Tuel, *J. Mol. Catal. A: Chem.*, 142 (1999) 361.
- [30] X. Wang, K.S.K. Lin, J.C.C. Chan, S. Cheng, *Chem. Commun.*, (2004) 2762.
- [31] J. Mondal, A. Modak, A. Bhaumik, *J. Mol. Catal. A: Chem.*, 335 (2011) 236.
- [32] A. Anan, K.K. Sharma, T. Asefa, *J. Mol. Catal. A: Chem.*, 288 (2008) 1.
- [33] S. Huh, J.W. Wiench, J.-C. Yoo, M. Pruski, V.S.-Y. Lin, *Chem. Mater.*, 15 (2003) 4247.
- [34] I.I. Slowing, B.G. Trewyn, V.S.-Y. Lin, *J. Am. Chem. Soc.*, 129 (2007) 8845.
- [35] H. Yang, G. Zhang, X. Hong, Y. Zhu, *Microporous Mesoporous Mat.*, 68 (2004) 119.
- [36] D.J. Kim, B.C. Dunn, P. Cole, G. Turpin, R.D. Ernst, R.J. Pugmire, M. Kang, J.M. Kim, E.M. Eyring, *Chem. Commun.*, (2005) 1462.
- [37] S. Meiboom, D. Gill, *Rev. Sci. Instrum.*, 29 (1958) 688.
- [38] J.W. Wiench, V.S.-Y. Lin, M. Pruski, *J. Magn. Reson.*, 193 (2008) 233.
- [39] R.K. Zeidan, M.E. Davis, *J. Catal.*, 247 (2007) 379.
- [40] K.B. Taylor, *Enzyme kinetics and mechanisms*, Kluwer Academic, 2002.
- [41] J. Wagner, R.A. Lerner, C.F. Barbas III, *Science*, 270 (1995) 1797.
- [42] T. Hoffmann, G. Zhong, B. List, D. Shabat, J. Anderson, S. Gramatikova, R.A. Lerner, C.F. Barbas III, *J. Am. Chem. Soc.*, 120 (1998) 2768.
- [43] N. Solin, L. Han, S. Che, O. Terasaki, *Catal. Commun.*, 10 (2009) 1386.
- [44] D.J. Cole-Hamilton, *Science*, 299 (2003) 1702.
- [45] J.D. Bass, A. Solovyov, A.J. Pascall, A. Katz, *J. Am. Chem. Soc.*, 128 (2006) 3737.
- [46] S. Huh, H.-T. Chen, J.W. Wiench, M. Pruski, V.S.-Y. Lin, *Angew. Chem. Int. Ed.*, 44 (2005) 1826.
- [47] L. Forni, G. Fornasari, G. Giordano, C. Lucarelli, A. Katovic, F. Trifiro, C. Perri, J.B. Nagy, *Phys. Chem. Chem. Phys.*, 6 (2004) 1842.
- [48] L. Forni, G. Fornasari, G. Giordano, C. Lucarelli, A. Katovic, F. Triflò, C. Perri, J.B. Nagy, Effect of exchange procedure and crystal size on high silica MFI zeolite as catalyst for vapor phase Beckmann rearrangement, in: M.C. E. van Steen, L.H. Callanan (Eds.) *Stud. Surf. Sci. Catal.*, Elsevier, 2004, 2823.
- [49] L.-P.B. Beaulieu, L.B. Delvos, A.B. Charette, *Org. Lett.*, 12 (2010) 1348.
- [50] D.W. Sindorf, G.E. Maciel, *Journal of Physical Chemistry*, 87 (1983) 5516.
- [51] V.H. Pan, T. Tao, J.-W. Zhou, G.E. Maciel, *J. Phys. Chem. B*, 103 (1999) 6930.

- [52] M.I. Zaki, M.A. Hasan, F.A. Al-Sagheer, L. Pasupulety, *Langmuir*, 16 (1999) 430.
- [53] J.H. Drese, A.D. Talley, C.W. Jones, *ChemSusChem*, 4 (2011) 379.
- [54] V.Y. Borovkov, A.V. Zaiko, V.B. Kazansky, W.K. Hall, *J. Catal.*, 75 (1982) 219.
- [55] I.D. Gay, *J. Phys. Chem.*, 78 (1974) 38.
- [56] T. Bernstein, D. Michel, H. Pfeifer, P. Fink, *J. Coll. Interface Sci.*, 84 (1981) 310.
- [57] S. Nedd, T. Kobayashi, C.-H. Tsai, I.I. Slowing, M. Pruski, M.S. Gordon, *J. Phys. Chem. C*, 115 (2011) 16333.
- [58] M.B. Schmid, K. Zeitler, R.M. Gschwind, *J. Am. Chem. Soc.*, 133 (2011) 7065.
- [59] H.E. Zimmerman, M.D. Traxler, *J. Am. Chem. Soc.*, 79 (1957) 1920.
- [60] S. Bahmanyar, K.N. Houk, *J. Am. Chem. Soc.*, 123 (2001) 11273.
- [61] A.C. Dash, B. Dash, D. Panda, *J. Org. Chem.*, 50 (1985) 2905.

Captions

Schemes

Scheme 1. Cross-aldol condensation between *p*-nitrobenzaldehyde **1** and acetone.

Scheme 2. Formation of a Schiff base between *p*-nitrobenzaldehyde substrate **1** and the aminopropyl group of AP-MSN.

Scheme 3. Possible pathway of proton transfer assisted by silanol groups.

Figures

Figure 1. Effect of substrate concentration on the rate of AP-MSN-3.6 catalyzed cross-aldol condensation. The drop in rate at high concentrations of **1** suggests substrate inhibition of the reaction.

Figure 2. Infrared (a) and ¹³C CPMAS NMR (b) spectra of AP-MSN-2.8 before (black) and after (blue) reaction with **1**. Infrared spectrum of **1** (red) is included as a reference.

Figure 3. Kinetics of aldol condensation between **1** and acetone catalyzed by AP-MSN-3.6 and MAP-MSN-3.5 in hexane at 60°C with 3 mol% catalyst.

Figure 4. ²⁹Si DPMAS spectra of MAP-MSN-3.5 before (bottom) and after (top) blocking silanol groups with HMDS. Appearance of M sites due to the attached silane matches the conversion of the Q₂ and Q₃ sites of the blocked groups to Q₃ and Q₄, respectively.[50]

Figure 5. Effect of proximity between silanol and amine groups on the conversion of *p*-nitrobenzaldehyde. Catalytic activities are compared for: (a) homogeneous N-methyl-propylamine, (b) homogeneous N-methyl-propylamine + heterogeneous MSN, (c) silanol-passivated HMDS-MAP-MSN-3.5, and (d) heterogeneous MAP-MSN-3.5.